Binary and Recoil Collisions in Strong Field Double Ionization of Helium

A. Staudte,[1,][*] C. Ruiz,[2] M. Schöffler,[3] S. Schössler,[3] D. Zeidler,[4] Th. Weber,[5] M. Meckel,[3] D. M. Villeneuve,[1]
P. B. Corkum,[1] A. Becker,[2] and R. Dörner[3]

[1]*National Research Council, 100 Sussex Drive, Ottawa, Ontario K1A 0R6, Canada*
[2]*Max-Planck-Institut für Physik komplexer Systeme, Nöthnitzer Strasse 38, 01187 Dresden, Germany*
[3]*Institut für Kernphysik, J. W. Goethe Universität Frankfurt, Max-von-Laue-Strasse 1, 60438 Frankfurt, Germany*
[4]*Carl Zeiss SMT AG, Rudolf-Eber-Strasse 2, 73447 Oberkochen, Germany*
[5]*Lawrence Berkeley National Laboratory, Berkeley, California 94720, USA*
(Received 14 May 2007; published 28 December 2007)

We have investigated the correlated momentum distribution of both electrons from nonsequential double ionization of helium in a 800 nm, 4.5×10^{14} W/cm^2 laser field. Using very high resolution coincidence techniques, we find a so-far unobserved fingerlike structure in the correlated electron momentum distribution. The structure can be interpreted as a signature of the microscopic dynamics in the recollision process. We identify features corresponding to the binary and recoil lobe in field-free $(e, 2e)$ collisions. This interpretation is supported by analyzing *ab initio* solutions of a fully correlated three-dimensional helium model.

Today, it is well established that for infrared wavelengths at intermediate intensities (10^{13}–10^{15} W/cm^2) the emission of more than one electron from an atom or molecule proceeds via the rescattering mechanism [1]. According to this picture, first one electron is excited by the field to the continuum, it is then accelerated and driven back to its parent ion by the oscillating field where it can supply energy to liberate a second or even more electrons. The last step of the mechanism can be considered as an internal laser assisted electron-impact ionization of the residual ion. From the field-free counterpart (e.g., [2,3]), it is well known that after an electron-electron encounter the electrons either leave the ionic potential without further interaction (binary collision) or the incident electron gets additionally backreflected by the ion (recoil collision).

The observation of the correlated momenta (k_a, k_b) of both electrons (a, b) has been shown to provide a solid basis for an analysis of the rescattering dynamics. In many experiments [4–9] a maximum was observed for the emission of both electrons in the same direction with similar momentum components parallel to the laser field ($k_a^{\parallel} = k_b^{\parallel}$). This seemingly well established maximum is supported by numerous theoretical results (e.g., [10–12]) but is in conflict with others [13–17] which predict a minimum.

We have performed a new high resolution and high statistics experiment on double ionization of helium. Unlike previous experimental work our enhanced resolution and statistics unveil a minimum along $k_a^{\parallel} = k_b^{\parallel}$ bearing strong resemblance to the theoretical work in [15]. Our experimental observations are qualitatively reproduced by results of calculations using a recently introduced fully correlated two-electron quantum model [18]. Analysis of the temporal evolution of the momentum distributions in

the *ab initio* calculations as well as simple classical estimations let us interpret the basic features of the momentum distribution in view of binary and recoil collisions.

Our experiment was performed using cold target recoil ion momentum spectroscopy (COLTRIMS) [19,20]. Ti:sapphire laser pulses (40 fs, 800 nm, 5 μJ, 100 kHz repetition rate) are focused to peak intensity of $(4.5 \pm 0.5) \times 10^{14}$ W/cm^2 into a supersonic ^{4}He gas jet. The peak intensity in the laser pulse was determined by calibrating the pulse energy-to-intensity relation using the radial ion and electron momentum in a separate experiment in circularly polarized laser pulses [21]. The result was verified by fitting the predictions of tunnel theory [22] to the He$^+$ momentum distribution parallel to the laser field.

Ions and electrons created in the focus are guided by a 1.6 V/cm electric and a 10.5 G magnetic field towards two large area microchannel plate detectors (Ø 80 mm) with delay line position encoding [23]. The polarization axis of the laser is parallel to the spectrometer field. In the following we present only the momenta along the polarization, i.e., momenta measured via the time of flight of ions and electrons. We detect the ion and one electron, and for a fraction of phase space of double ionization we also detect both electrons. We find a resolution (FWHM) of <0.08 a.u. parallel and <0.14 a.u. perpendicular to the laser polarization axis. To avoid any problems with the dead time of the electron detector, we generally calculate the second electron from the measured electron and ion momentum using momentum conservation.

We use a laser repetition rate of 100 kHz. This yielded a count rate of ≈ 3 kHz on the ion detector and ≈ 10 kHz on the electron detector including stray electrons and dark counts. The fraction of false coincidences, where the detected ion and electron originate from two different atoms ionized in the same laser pulse, was monitored in the single

ionization channel (compare Fig. 1 in [4]). We find that 7%
of electrons and ions do not obey momentum conservation,
i.e., are not from the same atom. The base vacuum in our
chamber was about 10^{-10} mbar. The remaining back-
ground of H_2^+ ions from the residual gas can be very
efficiently suppressed by our three-dimensional momen-
tum imaging. He^{2+} ions have a very narrow momentum
distribution perpendicular to the polarization (0.8 a.u.
FWHM). The H_2^+ ions from the residual gas in contrast
have a thermal momentum distribution (≈ 5 a.u. FWHM).
Therefore, selecting transverse He^+ momenta <0.8 a.u.
efficiently suppresses the H_2^+ background. Cold H_2 con-
tamination in the gas jet has been frozen out by cooling our
nozzle on a cryogenic cold head to ≈ 14 K. A small re-
maining contribution is still visible in Fig. 1(a). Its position
off the diagonal reflects the nuclear mass defect in helium.
A total of 10^9 events contained 10^5 valid coincidences of a
He^{2+} and at least one electron.

Figure 1(a) shows the final momentum correlation of the
two electrons along the polarization axis. Since both elec-
trons are indistinguishable, the data were symmetrized by
exchanging the two electron indices. The first and third
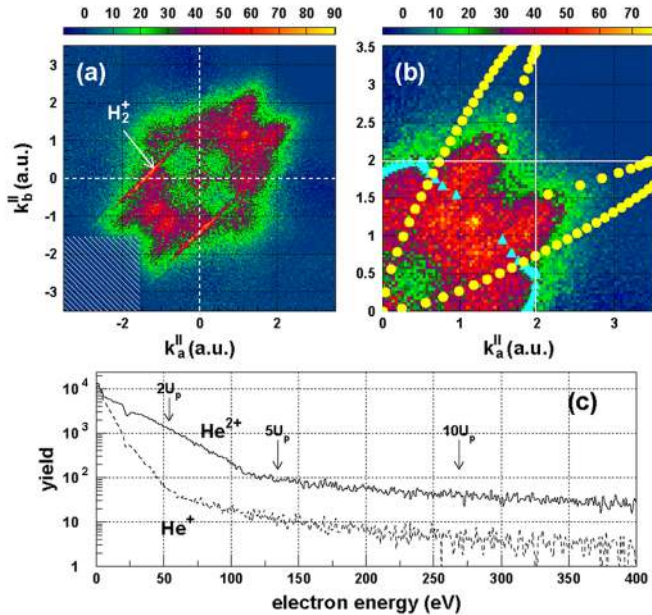quadrants thus correspond to events where both electrons

FIG. 1 (color online). (a) Correlated electron momenta for
double ionization of helium at 800 nm, 4.5×10^{14} W/cm^2.
Shown are the momentum components $k_{a,b}^{\parallel}$ along the polariza-
tion direction. Quadrants 1 and 3 correspond to both electrons
traveling into the same hemisphere. The indicated lines are H_2^+
background from cold H_2 in our gas jet. All other background
has been subtracted. (Hatched area) Detection limit for $k_{a,b}^{\parallel}$ away
from the electron detector. (b) Same as (a), only 1st quadrant is
shown, superimposed are the results of a classical $(e, 2e)$ scat-
tering model (see text for details). (Solid lines) $2\sqrt{U_p}$ cutoff
momentum for tunneled electrons. (c) Electron energy spectrum
of He^{2+} and He^+ (normalized to He^{2+}).

are detected in the same hemisphere, while the second and
fourth quadrants relate to final electron momenta that are
pointing back-to-back. We find a striking fingerlike struc-
ture producing a minimum along the diagonal of equal
momenta.

What is the origin of the fingerlike structure? At first
glance one realizes that the structure extends beyond the
limit of $2\sqrt{U_p}$ [white solid lines in Fig. 1(b)], which is the
classical limit expected for a joint emission of both elec-
trons upon a binary collision at the zero of the field. Here
$U_p = I/4\omega^2$ is the ponderomotive potential determined by
the intensity I and frequency ω of the field (atomic units
are used throughout this Letter unless otherwise indicated).
This enhancement in the production of hot electrons com-
pared to an uncorrelated model becomes even more strik-
ing in Fig. 1(c). Here, the electron energy spectrum of
He^{2+} is compared to the single ionization channel. Only
electrons emitted towards the electron detector ($k^{\parallel} \geq 0$)
are included. Hence, we anticipate that an electron with
final momentum beyond the classical limit has interacted
with the nucleus. Such a process is well known in field-free
$(e, 2e)$ processes as recoil collision. To gain insight, we
have determined the kinematical constraints in correlated
momentum space for various $(e, 2e)$ scenarios using a
simple classical model.

Our classical one-dimensional model neglects the parent
ion potential as well as the long-range electron-electron
repulsion. In the scenario of a binary collision, the mo-
mentum direction of the recolliding electron is unchanged.
For a recoil collision, the direction of the momentum of the
first electron is inverted (i.e., the electron is scattered by
180°). In both scenarios the impact energy of the recollid-
ing electron is reduced by the binding energy and the
second electron is born with zero momentum.

In Fig. 1(b) we have superimposed the kinematical con-
straints obtained from the classical model for the binary
collision (circles) and for the recoil collision (triangles)
with the experimental data of the first quadrant. The com-
parison reveals a strong correspondence between the fea-
tures seen in the experimental data and the classical
estimations. The binary collision scenario leads to a broad
distribution. But more interestingly, the estimations based
on a recoil collision exhibit the prominent fingerlike struc-
ture beyond the limit of $2\sqrt{U_p}$.

The assumed asymmetric energy sharing of the excess
electron-impact energy is typical in field-free $(e, 2e)$ pro-
cesses [24]. It also yields the best correspondence with the
experimental data compared to a more symmetric energy
sharing. Classical estimates including excited states of the
He^+ ion have shown that recollision excitation with sub-
sequent tunneling ionization (RESI) [5] is not responsible
for the fingerlike structure.

Next, we show that the results of our classical analysis
are supported by quantum mechanical calculations. To this
end, we have performed *ab initio* numerical simulations

using a recently introduced helium model [18], in which
the center-of-mass motion of the two electrons is restricted
to the polarization axis, while the electron correlation is
fully retained via the relative coordinate of the electrons.

In our simulation the coupling to the laser field is done
using the velocity gauge and within the dipole approxima-
tion. We have used an artificial laser pulse with a linear
ramp over two cycles to the peak intensity of 5×10^{14} W/cm^2 at 800 nm where it was kept constant for
two more oscillations of the field [see Fig. 2(a)]. The initial
wave function has been obtained via imaginary time propa-
gation and has been propagated using the Crank-Nicholson
method on a grid with $3000 \times 1500 \times 400$ points, other
grid parameters were as in [18].

In the simulation a restriction to a few oscillations of the
laser field is necessary in order to keep the full wave
function on the grid for a determination of the momentum
distribution at the end of the calculation. This requires a
large amount of computer resources (in time as well as in
memory), which quickly grows with the number of cycles
of the pulse. In fact, the proposed mechanism requires the
analysis of only a single rescattering event shortly after the
impact, without the obscuring contributions from earlier
rescattering events. The latter is achieved by the fast turn
on of the field.

In Fig. 2 we show the distribution of the correlated two-
electron momentum components along the polarization
direction at some time during the pulse [2(b)] and at the
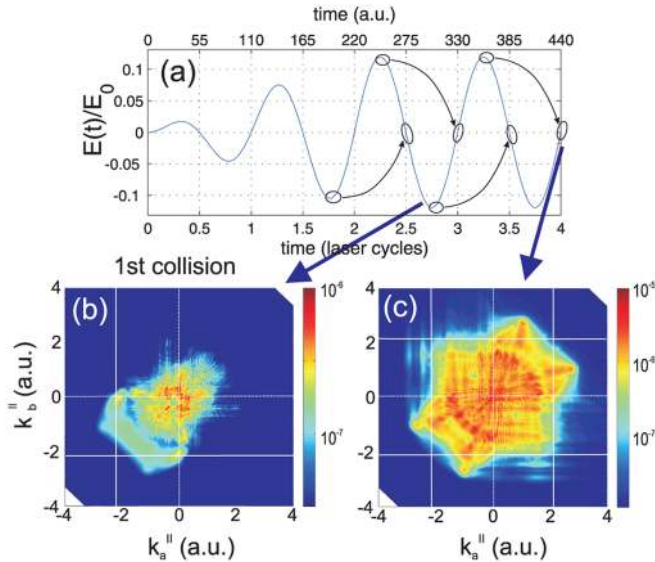end of the pulse [2(c)]. The distributions are obtained by

FIG. 2 (color online). Results of an *ab initio* quantum me-
chanical simulation using a helium model atom interacting with
a 4 cycle laser pulse at 800 nm and a peak intensity of
5×10^{14} W/cm^2 (a). Correlated two-electron momentum distri-
bution on a logarithmic scale (b) after the first significant
recollision and (c) at the end of the pulse. (Solid lines) $2\sqrt{U_p}$
corresponding to the vector potential at the instant of collision.

partitioning the coordinate space, extracting the double
ionization part of the wave function (cf. [18]), taking its
Fourier transform, and integrating over the direction per-
pendicular to the field. Note that these distributions corre-
spond to the canonical momenta $\mathbf{p} = -i\hbar\nabla$ of the two
electrons, which correspond in this case to the momentum
to be observed outside the field at the detector.

The emission of the two electrons primarily into the
same hemisphere as a key signature of a recollision event,
as well as a fingerlike structure, are nicely reproduced in
the final momentum distribution [Fig. 2(c)]. As in the
experimental data, the fingerlike structure extends beyond
the limit of $2\sqrt{U_p(t_{\text{rec}})}$ [solid lines in Figs. 2(b) and 2(c)].
Differences in the orientation of the fingerlike structure, as
compared to the experimental data, are probably due to the
dimensional reduction of the two-electron Hamiltonian in
the simulation. The momentum distribution obtained dur-
ing the pulse [Fig. 2(b)] is due to the first major rescattering
event at about $t_{\text{rec}} \approx 275$ a.u. We may note parenthetically
that the interferences between the contributions from the
different pathways in the final momentum distribution are
signatures of the quantum nature of the double ionization
process.

As the momentum distribution in the third quadrant
[Fig. 2(b)] corresponds mainly to a single rescattering
event at $t = 275$ a.u., we are in the position to further
analyze it in view of contributions from binary and recoil
collisions. To this end we have obtained partial canonical
momentum distributions from different spatial configura-
tions of the two electrons. The results are shown in Fig. 3.
For the distribution in Fig. 3(a) we have restricted the
double ionization coordinate space to electron pairs found
in that hemisphere, which corresponds to an emission of
both electrons in the direction of the incident electron in
the recollision. As discussed above, this emission pattern is
a signature of the binary collision scenario. The corre-
sponding momentum distributions confirm that for a binary
collision the maximum appears for $k_a^{\parallel} = k_b^{\parallel}$. For the results
shown in Fig. 3(b) the coordinate space has been restricted
to two electrons leaving the ion into opposite hemispheres.
The canonical momentum distribution obtained from this
configuration beyond the $2\sqrt{U_p}$ limit has a minimum for
both electrons with equal final momentum. Hence, the
results of the quantum mechanical simulation strongly
support our interpretation that a recoil collision gives rise
to the observed fingerlike structure.

Because of the influence of the external field on the
emitted electrons the above analysis is imperfect, as can
be seen from the fact that contributions in Figs. 3(a) and
3(b) do not fully reconstruct the total momentum distribu-
tion in Fig. 2(b). Part of the two-electron continuum wave
function, created early in the rescattering event, is redis-
tributed by the field into the hemisphere opposite to the
direction of the incident electron (field direction). As can
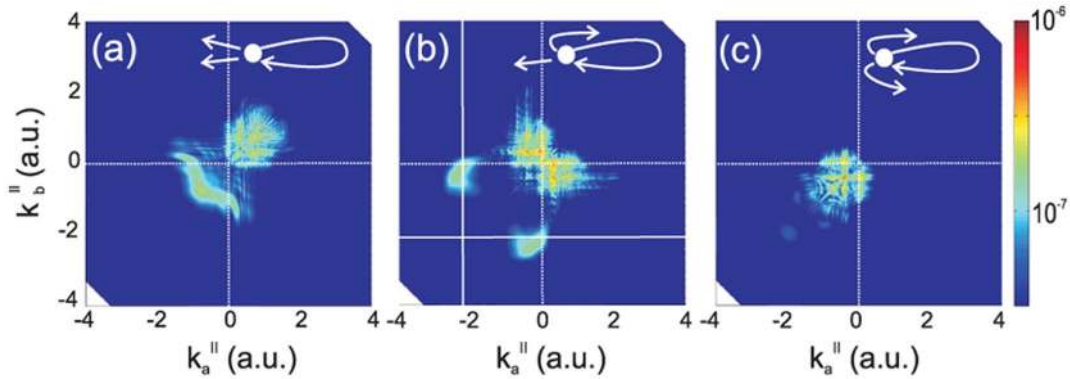be seen from Fig. 3(c) these contributions provide the

FIG. 3 (color online). Partial two-electron momentum distributions (on logarithmic scale) shortly after the first recollision ($t_{rec} \approx$ 275 a.u.) for (a) two electrons parallel in the same direction as the incident electron, (b) two electrons in back-to-back direction, and (c) both electrons opposite to the direction of the incident electron. (Solid lines) Maximum drift momentum $2\sqrt{U_p}$.

remaining part of the full momentum distribution. They consist of contributions of both the binary and the recoil recollisions.

In conclusion our experiment on strong field double ionization of helium shows a fingerlike structure in the correlated electron emission. This unveils novel details of the rescattering dynamics establishing a close correspondence between field-free and field-assisted $(e, 2e)$ collision. Classical estimations and *ab initio* results from a fully correlated helium model show that these fingers results from electron-impact ionization with backscattering at the nucleus upon recollision, an analogue to the recoil peak in field-free $(e, 2e)$ collisions.

*andre.staudte@nrc.ca

[1] P. B. Corkum, Phys. Rev. Lett. **71**, 1994 (1993).
[2] T. Rösel, J. Röder, L. Frost, K. Jung, and H. Ehrhardt, J. Phys. B **25**, 3859 (1992).
[3] J. Berakdar, J. Röder, J. S. Briggs, and H. Ehrhardt, J. Phys. B **29**, 6203 (1996).
[4] Th. Weber, H. Giessen, M. Weckenbrock, G. Urbasch, A. Staudte, L. Spielberger, O. Jagutzki, V. Mergel, M. Vollmer, and R. Dörner, Nature (London) **405**, 658 (2000).
[5] B. Feuerstein *et al.*, Phys. Rev. Lett. **87**, 043003 (2001).
[6] E. Eremina, X. Liu, H. Rottke, W. Sandner, A. Dreischuh, F. Lindner, F. Grasbon, G. G. Paulus, H. Walther, R. Moshammer, B. Feuerstein, and J. Ullrich, J. Phys. B **36**, 3269 (2003).
[7] R. Moshammer, J. Ullrich, B. Feuerstein, D. Fischer, A. Dorn, C. D. Schröter, J. R. Crespo López-Urrutia, C. Höhr, H. Rottke, C. Trump, M. Wittmann, G. Korn, K. Hoffmann, and W. Sandner, J. Phys. B **36**, L113 (2003).
[8] E. Eremina, X. Liu, H. Rottke, W. Sandner, M. G. Schätzel, A. Dreischuh, G. G. Paulus, H. Walther, R. Moshammer, and J. Ullrich, Phys. Rev. Lett. **92**, 173001 (2004).
[9] D. Zeidler, A. Staudte, A. B. Bardon, D. M. Villeneuve, R. Dörner, and P. B. Corkum, Phys. Rev. Lett. **95**, 203003 (2005).
[10] J. Chen, J. Liu, L. B. Fu, and W. M. Zheng, Phys. Rev. A **63**, 011404 (2000).
[11] A. Becker and F. H. M. Faisal, Phys. Rev. Lett. **89**, 193003 (2002).
[12] S. L. Haan, L. Breen, A. Karim, and J. H. Eberly, Phys. Rev. Lett. **97**, 103008 (2006).
[13] M. Lein, E. K. U. Gross, and V. Engel, Phys. Rev. Lett. **85**, 4707 (2000).
[14] C. Figueira de Morisson Faria, H. Schomerus, X. Liu, and W. Becker, Phys. Rev. A **69**, 043405 (2004).
[15] J. S. Parker, B. J. S. Doherty, K. T. Taylor, K. D. Schultz, C. I. Blaga, and L. F. DiMauro, Phys. Rev. Lett. **96**, 133001 (2006).
[16] J. S. Prauzner-Bechcicki, K. Sacha, B. Eckhardt, and J. Zakrzewski, Phys. Rev. Lett. **98**, 203002 (2007).
[17] Phay J. Ho, Phys. Rev. A **72**, 045401 (2005).
[18] C. Ruiz, L. Plaja, L. Roso, and A. Becker, Phys. Rev. Lett. **96**, 053001 (2006).
[19] R. Dörner, V. Mergel, O. Jagutzki, L. Spielberger, J. Ullrich, R. Moshammer, and H. Schmidt-Böcking, Phys. Rep. **330**, 95 (2000).
[20] J. Ullrich, R. Moshammer, A. Dorn, R. Dörner, L. Ph. H. Schmidt, and H. Schmidt-Böcking, Rep. Prog. Phys. **66**, 1463 (2003).
[21] A. Alnaser, X. M. Tong, T. Osipov, S. Voss, C. M. Maharjan, B. Shan, Z. Chang, and C. L. Cocke, Phys. Rev. A **70**, 023413 (2004).
[22] N. B. Delone and V. P. Krainov, Phys. Usp. **41**, 469 (1998).
[23] O. Jagutzki, V. Mergel, K. Ullmann-Pfleger, L. Spielberger, U. Spillmann, R. Dörner, and H. Schmidt-Böcking, Nucl. Instrum. Methods Phys. Res., Sect. A **477**, 244 (2002).
[24] T. W. Shyn, Phys. Rev. A **45**, 2951 (1992).